Electromagnetic Properties of YIG Polycrystalline Ceramics Fabricated by Tape-casting Method①

ZHAO Chong[a] YE Wang-Gui[a] LI Ying-Kui[b] SHEN Xiao-Fei[b]
CAO Zhi-Jun[c] CAO Zhi-Quan[d] WEN Zi-Cheng[b, e]
YUAN Xuan-Yi[a] MA Chao-Yang[b②] CAO Yong-Ge[b, e②]

[a] (*Department of Physics, Renmin University of China, Beijing* 100872, *China*)
[b] (*Songshan Lake Materials Laboratory, Dongguan* 523808, *China*)
[c] (*University of Virginia, Charlottesville, VA* 22904, *USA*)
[d] (*New York University, New York, NY* 10003, *USA*)
[e] (*Institute of Physics, Chinese Academy of Sciences, Beijing* 100190, *China*)

ABSTRACT Pure phase $Y_3Fe_5O_{12}$ (YIG) ceramic was successfully produced by tape-casting forming process and one-step solid-state sintering method. The activation energy for densification was calculated to be 183.81 kJ/mol. Pure YIG ceramic with a relative density as high as 99.8% was fabricated. The existence of O vacancy and Fe^{2+} ions was determined by XPS and EPR spectra. The RT saturation magnetization was measured to be 28.2 emu/g, and the hysteresis loss was calculated to be smaller than 10 mJ/kg in the temperature range of 230 ~ 360 K and be as high as 238.8 mJ/kg at 30 K. The dielectric loss tangent $\tan\delta_\varepsilon$ was nearly zero at 6 ~ 7 GHz and 11 ~ 12 GHz. For complex permeability in the frequency range of 5 ~ 18 GHz, the magnetic loss tangent $\tan\delta_\mu$ fluctuated at around zero. Therefore, the low values of $\tan\delta_\varepsilon$ and $\tan\delta_\mu$ indicate that it is a low loss ceramic material.

Keywords: YIG ceramic, tape-casting, microwave, hysteresis loss, magnetodielectric ceramic;
DOI: 10.14102/j.cnki.0254–5861.2011–3034

1 INTRODUCTION

Yttrium iron garnet, $Y_3Fe_5O_{12}$ (YIG), has a bcc cubic structure and belongs to space group *Ia*-3*d* (230). Furthermore, per unit cell (1895.6 $Å^3$) contains 8 formula units, where Y^{3+} ions occupy the eight-coordinate (O^{2-}) dodecahedral sites, while Fe^{3+} ions partially take up six-coordinate octahedral and three-coordinate tetrahedral sites. YIG materials and its modifications by doping as soft ferrites are suitable for magnetic microwave devices with high frequency and low microwave loss[1]. Microwave filters and oscillators based on YIG have a wider electric tuning range in frequency than other candidates including ferroelectric and varactors[2]. Multiferroic magnetoelectric materials developed on YIG exhibit both ferroelectricity and ferromagnetism, and typically yield much larger magnetoelectric coupling response than natural multiferroic single-phase compounds, making them suitable for magneto-electric applications[3]. Faraday rotators with substituted YIG films or bulk crystals own large Faraday Rotation capacity, low saturation magnetization and low optical absorption loss, showing high potential applications in magneto-optical devices[4, 5].

Pure polycrystalline Bi-substituted YIG thin films were grown on corning glass substrates by an original CVD technique and its Faraday rotation properties were studied[6]. Bi-substituted Y–Yb mixed iron garnet single crystals were grown by the flux method and the specific Faraday Rotation, optical absorption coefficient and the saturation magnetization were investigated[4]. Nowadays, polycrystalline YIG (powder or bulk ceramic) is generally synthesized through conventional solid-state reaction (CSSR) method. For YIG ceramic, properties of density, purity and microstructure have great impact on the magnetic properties and therefore the performance of its microwave devices. However, some secon

Received 9 November 2020; accepted 27 January 2021

① This project was supported by the National Key R&D Program of China (2017YFB0403200) and the National Natural Science Foundation of China (No. 51872327)

② Corresponding authors. Ma Chao-Yang, Ph.D., an associate researcher at Songshan Lake Materials Laboratory. E-mail: machaoyang@sslab.org.cn;
Cao Yong-Ge, Ph.D., full researcher at Songshan Lake Materials Laboratory. E-mail: caoyongge@sslab.org.cn

dary phases (Fe_2O_3, $YFeO_3$, YFe_2O_4) usually coexist with YIG fabricated by CSSR method[7, 8]. The growth kinetic and reaction mechanisms of Y_2O_3–Fe_2O_3 system were studied by different diffusion couples. And the results showed that the formation of YIG phases was highly dependent on pre-formed YIP phases and the diffusion of Fe^{3+} cations[9-11]. By adding excess 8 ~ 10 wt% Fe_2O_3, 99% of YIG ceramic phase was achieved. What's more, YIG with properly excess Fe_2O_3 could be used for high frequency tunable dielectric resonator antenna (DRA)[12, 13]. Recently, YIG ceramic with about 98 ~ 99% of theoretical density was fabricated by solid-state reaction method[14, 15], while new fabrication methods are pursued for much higher dense and purely fine-grained YIG ceramic.

In this work, high-dense pure YIG polycrystalline ceramic was fabricated by tape-casting forming process and one-step solid-state reaction method. Phase purity, relative density and micro-morphology dependent on sintering temperature and holding time were studied. The activation energy was calculated from the linear Arrhenius plots. XPS was performed to check valance states of Fe and O atoms, as well as EPR spectrum was introduced to check O vacancy. Thereafter, magnetic and dielectric properties were chracta-rized for the sample sintered at 1400 ℃ for 8 h.

2 EXPERIMENTAL

Commercially available powders of Y_2O_3 (99.99%, 5.9 μm, Jiangyin Jiahua Advanced Material Resources Co., Ltd., China) and Fe_2O_3 (99.99%, 5 ~ 10 μm, Aladdin, China) were used as raw materials without further purification. Powders were precisely weighted in accordance with the stoichiometry of $Y_3Fe_5O_{12}$ and then added into the mixed solvent of 40 wt% ethanol and 60 wt% xylene with the weight ratio of powders to solvent at 3:2. Besides, 0.4 wt% TEOS (tetraethyl orthosilicate) as sintering aid and 4 wt% fish oil as dispersant were put into the mixture. Then, the mixed slurry was planetary ball-milled for 24 h. Subsequently, binder (6 wt% polyvinyl butyral), plasticizers (3 wt% polyalkylene glycol & 3 wt% butyl benzyl phthalate) and defoamers (3 wt% n-butyl alcohol & 3 wt% ethylene glycol) were added and ball-milled for another 24 h.

Thereafter, the tape-casting forming process was carried out. The distance between the blade and tape was 500 μm and the casting speed was 500 mm/min. The prepared slurry on the tape was dried at room temperature, and then cut into slices. Six or eight layers of slices were stacked and compressed under 20 Mpa at 120 ℃ to form into green body which was calcined at 800 ℃ in an oxygen atmosphere to remove organic additives, and then sintered at various temperature in a furnace under air atmosphere. Finally, the obtained YIG ceramic was prepared for characterization.

The phase identification of the fabricated ceramic was performed on an XRD system (Bruker, Germany) using Cu$K\alpha$ radiation (λ = 1.5406 Å). The surface micro-morphology was carried on a field-emission SEM (JSM-6700F, JEOL, Japan). The XPS was conducted by using an X-ray photoelectron spectrometer (ESCALAB 250X, Thermo Scientific, USA). The EPR was conducted by using an electron paramagnetic resonance instrument (A300-10/12, Bruker, Germany). The bulk density was measured using the Archimedes' method. The magnetic hysteresis loops were obtained by a vibrating sample magnetometer (VSM, QD, USA). The magnetic and dielectric properties were determined with a microwave network analyzer (PNA-N5244A, Agilent, USA).

3 RESULTS AND DISCUSSION

3. 1 XRD

Fig. 1 shows the XRD patterns of YIG ceramic fabricated by combining tape-casting forming process and solid-state reaction method at various sintering temperature in air atmosphere. Clearly, the ceramic with sintering temperature above 1100 ℃ is all YIG pure phases (PDF# 71-2150). According to Ali's report, YIG ceramic prepared through dry-pressing forming process generally contains unwanted phase of YIP even with 1250 ℃ sintering temperature[9]. It is suggested that YIP is formed as an intermediate phase and will further react with Fe_2O_3 to produce single-phase YIG by diffusion process[11], and Fe^{3+} cations diffuse and initiate the Fe–Y atomic bonding. Then, with Fe^{3+} cations continuously diffusing, the YIP layer covered on the surface of Y_2O_3 particles turned to be YIG while the inner Y_2O_3 changed into YIP. Considering the saturated vapor pressure of Fe and Y calculated by Eq. (1) and listed in Table 1, Fe has a larger saturated vapor pressure than Y, which signifies that the iron is more volatile in this system. If Fe_2O_3 is inhomogeneous in this system, high concentration of Fe element means more evaporation at high temperature. Therefore, the existence of YIP impurity highly depends on the inhomogeneity and evaporation of Fe_2O_3. Compared with the dry-pressing forming method, our tape-casting forming method provides

much better homogeneous mixture of Y_2O_3 and Fe_2O_3 particles, thus leading to the highly pure YIG ceramic.

$$log(p/atm) = A + B/T + C \times log(T) + D/T^3 \quad (1)$$

Here, coefficients in the equation can be obtained from reference[16] and listed in Table 1.

Table 1. Vapor Pressure of Metallic Elements Fe and Y in the Solid State at about 1800 K

Element	A	B	C	D	T(melt)/K	P/atm
Fe	7.1	–21723	0.4536	–0.5846	1808	3.652×10^{-4}
Y	9.735	–22306	–0.8705	0	1799	2.967×10^{-6}

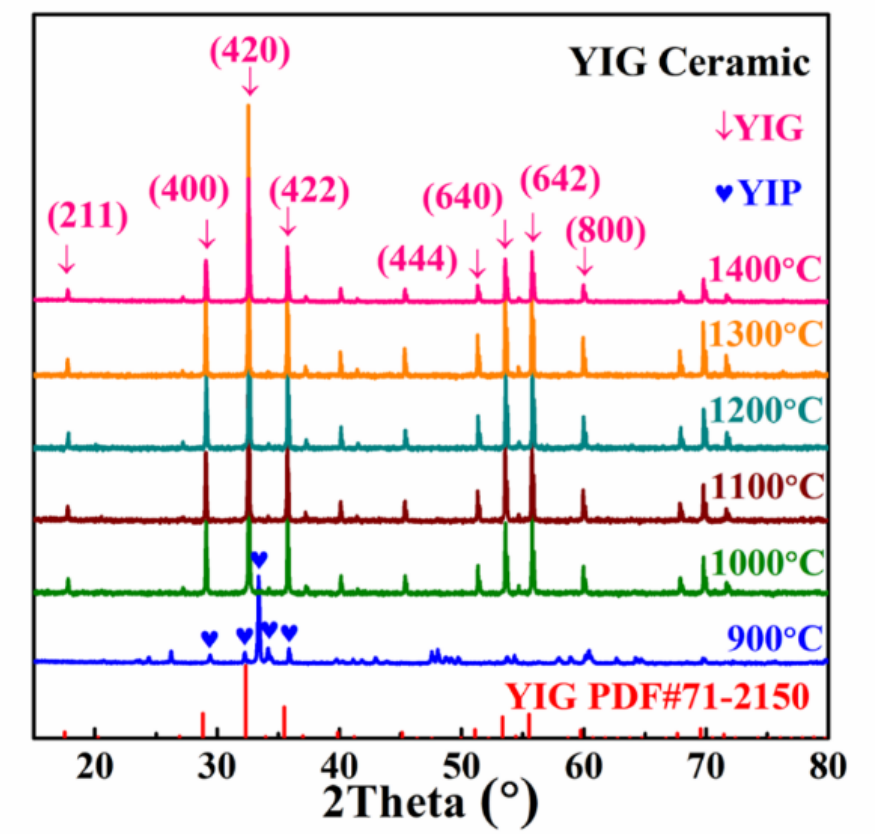

Fig. 1. XRD patterns of YIG ceramic sintered under various temperature in air atmosphere

3. 2 SEM and XPS

Figs. 2a ~ 2f show the SEM images of YIG ceramic prepared at various sintering temperature for 10 h and the evolution of morphologies is in agreement with the Ostwald ripening process. Along with the sintering temperature increasing from 900 to 1400 ℃, driven by the sintering kinetics, few grains gradually adhere to each other with grain boundaries and grow to be big grains to reduce the interfacial area. As a result, gaps and pores between grains are gradually eliminated at the same time. Samples sintered at 1400 ℃ exhibit no pores exist in both grains and boundaries, indicating a quite high densification, as discussed in Section 3. 3. Grain size in Fig. 4f is non-uniform and varies from several microns to several dozens of microns, which can be ascribed to the asynchronous growth of grains at different regions and thereof migration of grain-boundaries, as shown in Figs. 2a ~ 2e.

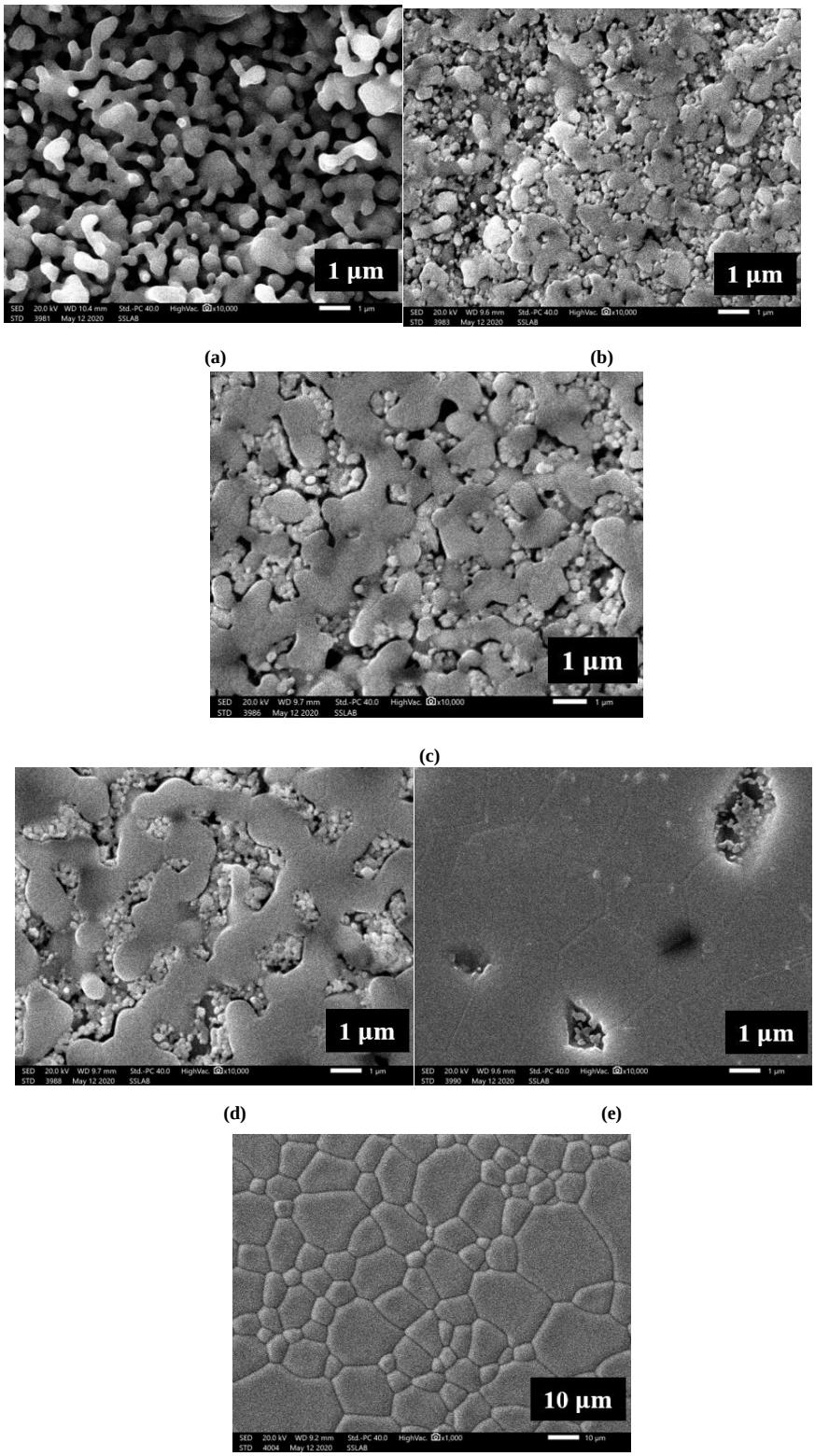

Fig. 2. SEM images of YIG ceramic sintered at (a) 900 ℃, (b) 1000 ℃, (c) 1100 ℃, (d) 1200 ℃, (e) 1300 ℃ and (f) 1400 ℃ for 10 h

According to Chen's report, Fe^{2+} ions and oxygen vacancies may exist in ceramic fabricated by high temperature sintering process due to the low oxygen conditions[15], and this can be verified by XPS measurement. Fig. 3 shows XPS spectra of YIG ceramic sintered at 1400℃ for 10 h. The XPS spectrum confirmed the existence of Fe $2p_{1/2}$, Fe $2p_{3/2}$, Fe 3*s*, Fe 3*p*, O 1*s*, O 2*s*, Y 3*s*, Y $3p_{1/2}$, Y $3p_{3/2}$, C 1*s*, Y 3*d*, Y 4*s* and Y 4*p* signals for the sample as shown in Fig. 3a. In Fig. 3b, based on the Lorentzian-Gaussian fitting, Fe $2p_{3/2}$ and Fe $2p_{1/2}$ peaks can both be divided into Fe^{3+} and

Fe^{2+} peaks centered at 711.6, 726.4, 710.2 and 724.2 eV. Meanwhile, O 1s spectrum in Fig. 3c is divided into two peaks centered at 529.9 and 531.6 eV, and the latter one indicated the existence of oxygen vacancy which can also be proved by the EPR spectrum, as shown in the illustration in Fig. 3c.

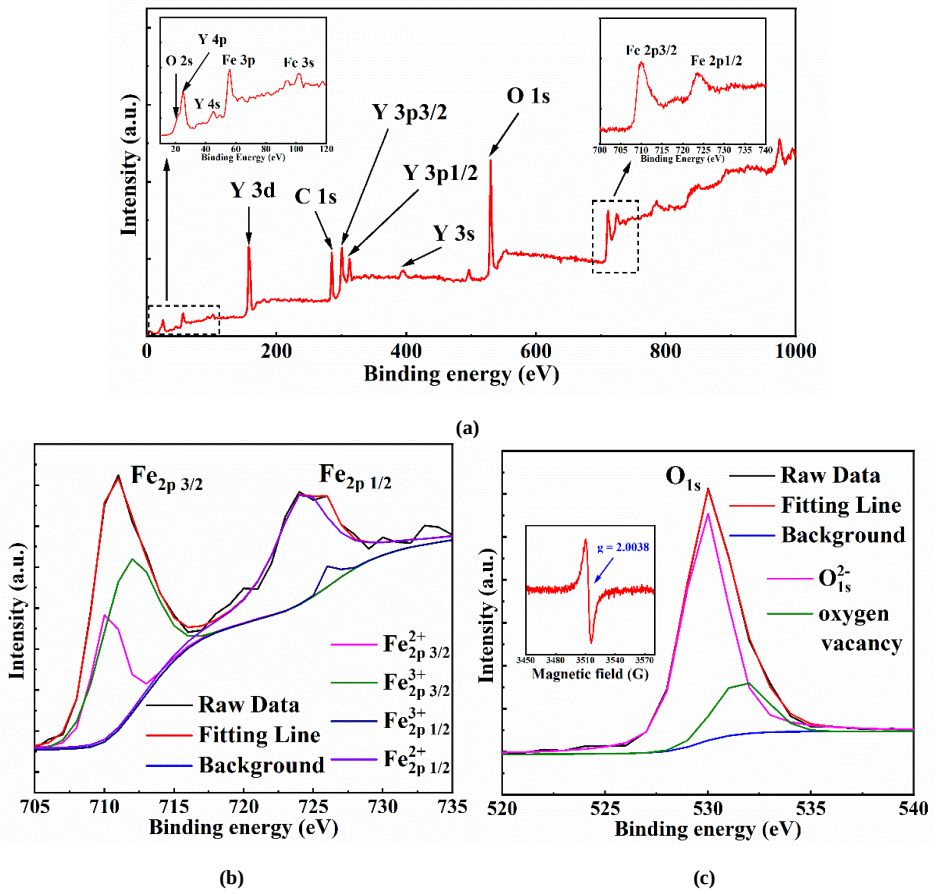

Fig. 3. XPS spectra in (a) the survey range, (b) Fe ion and (c) O ion in YIG ceramic sintered at 1400 ℃ for 10 h. The EPR spectrum as inset

3. 3 Relative density and activation energy

The sintering kinetics, namely densification kinetics, of YIG ceramic could be characterized by the relationship between the relative density and sintering conditions (temperature and holding time). Densities of YIG ceramic sintered at various temperature and holding time was measured by Archimedes' method and plotted in Fig. 4a. Obviously, higher sintering temperature and longer holding time did lead to higher relative density. Besides, the relative density increased significantly along with the temperature below 1375 ℃, while slowly when the temperature was further raised. For samples sintered at 1450 ℃ for 8 h, the relative density reached the highest value of 99.8%, which was bigger than that values reported in references[14, 17]. The high relative density indicated extremely low residual porosity and highly dense microstructure. Densification kinetics can be interpreted by Arrhenius equation[9, 17]:

$$\ln K = -E_a/RT + C$$

where, E_a is the activation energy for YIG ceramic densification, R the gas constant (8.314 J/mol/K), T the absolute temperature, C the constant, and K the rate constant depending on temperature. Densification rate versus reciprocal temperature is plotted in Fig. 4b, where rate constant K was related to the relative density and calculated from Fig. 4a. By linear fitting, the value of E_a was determined to be 183.81 kJ/mol, which was comparable with the activation energy of 169 kJ/mol for lattice diffusion or grain boundary formation[17] and much smaller than the energy of 484 kJ/mol for YIG formation from YIP[9]. It can be drawn that the mechanisms of YIG phase formation and ceramic densification were the result of homogeneous diffusion probably assisted by the sintering aids of SiO_2 (products of TEOS decomposition) located at grain boundaries.

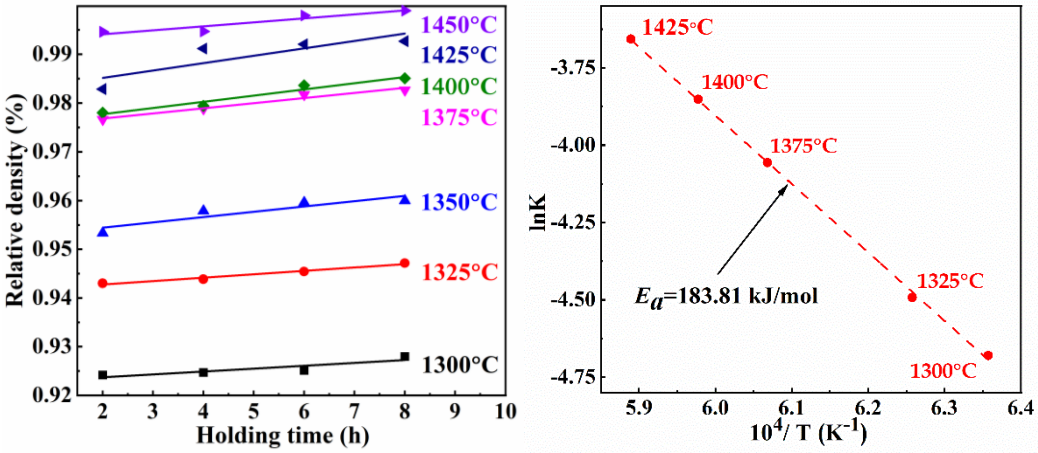

(a) (b)

Fig. 4. (a) Relative densities of YIG ceramic sintered at various temperature and holding time. (b) Activation energy analysis for YIG ceramic

3. 4 Intrinsic magnetic property

The magnetic properties of YIG ceramic sintered at 1400 ℃ were studied by the static hysteresis loops under various temperature (Fig. 5a). The well-defined hysteresis loop can be clearly observed at 30 K, while turned to be narrower along with the increase of temperature. The saturation magnetization (M_s) and hysteresis loss (area of the hysteresis loop) depending on temperature are plotted in Fig. 5b. The value of M_s decreased from 38.9 emu/g down to 25.3 emu/g from 30 K up to 360 K. And, the trend could be ascribed to the enhanced thermal vibrations of atoms and lattices under high temperature, and hence magnetic dipoles were difficult to be aligned[18]. It was worth mentioning that the room-temperature (300 K) value of M_s was 28.2 emu/g, which is a little higher than 27.4 emu/g reported in previous literature[14]. The result indicated that our YIG ceramic exhibited much higher relative density and more compact microstructures. Hysteresis loss, characterized by the area of the hysteresis loop, generally decreased with temperature. However, in this work, there is an upturn point at 230 K (4 mJ/kg), and the mechanism needed to be further studied. Besides, hysteresis loss at 30 K was as high as 238.8 mJ/kg, while values at 230 ~ 360 K are smaller than 10 mJ/kg.

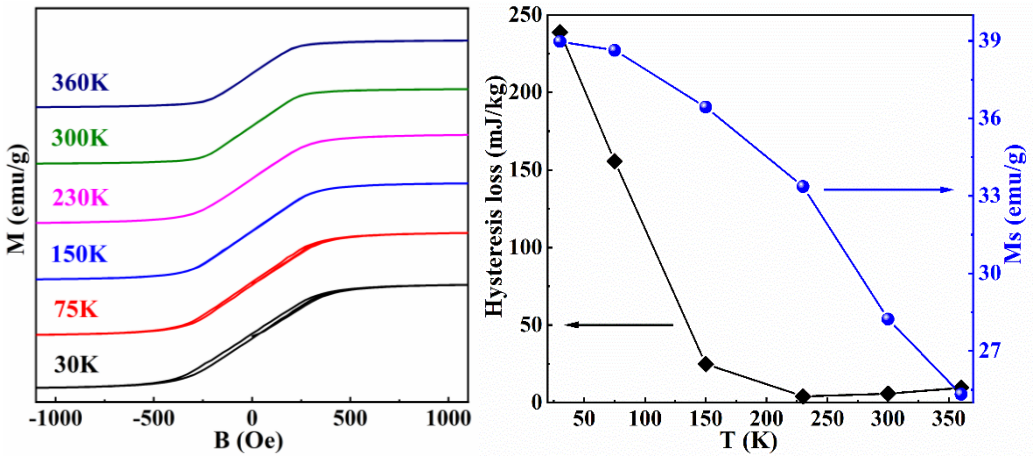

(a) (b)

Fig. 5. (a) Magnetic hysteresis loops and (b) M_s and hysteresis loss of YIG ceramic sintered at 1400 ℃ for 8 h at various test temperature

3. 5 Electromagnetic parameters

Fig. 6 shows the zero-field complex permittivity properties of home-made YIG ceramic circle (The fabricated YIG ceramic was grinded into powder, homogenously mixed with paraffin by a mass ratio of 3:7, and thereafter formed into a 2 mm thickness circle with an inner diameter of 3 mm and an

outer diameter of 7 mm). Along with the frequency increasing from 2 to 18 GHz, the changing trends of real part ε' (the ability for the storage of electrical energy) and the imaginary part ε'' (the dissipation capacity of electrical energy) are just opposite, and some relaxation peaks are clearly observed as a result of the multiple relaxation processes, as shown in Fig. 6a[19]. In addition, the dielectric loss tangent $\tan\delta_\varepsilon$ determined by $\varepsilon''/\varepsilon'$ fluctuates with the frequency, and interestingly, $\tan\delta_\varepsilon$ at about 6 ~ 7 and 11 ~ 12 GHz is extremely low suitable for practical microwave devices (Fig. 6b). As we know, the dielectric loss is ascribed to the conduction loss and polarization relaxation loss. And, polarization relaxation loss can be characterized by the Cole-Cole semicircle, that is, a simple semicircle in the $\varepsilon'\varepsilon''$-coordinate plane means a polarization relaxation process. As shown in Fig. 6c, the three semicircles suggest that the dielectric loss is determined by multiple dielectric relaxation loss, which is in accordance with the relaxation peaks in Fig. 6a[20]. Future work will be focused on the dielectric properties of YIG ceramic under applied magnetic field in a wide range of frequency.

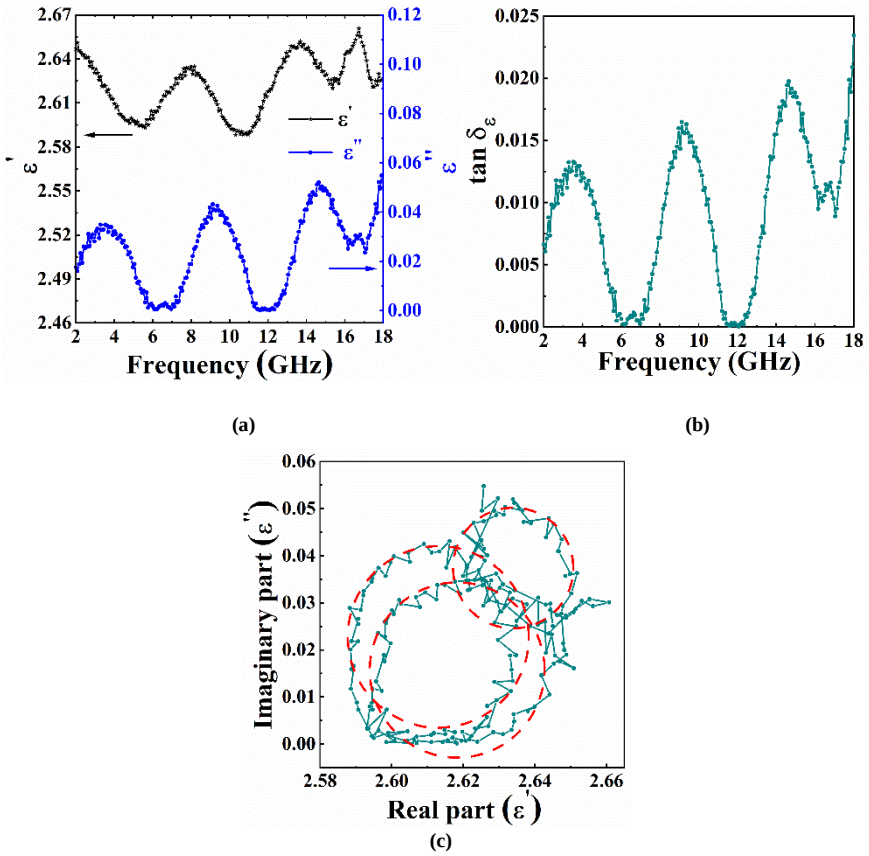

Fig. 6. Frequency dependence of (a) ε' and ε'', (b) $\tan\delta_\varepsilon$, and (c) Cole-Cole semicircle of YIG ceramic sintered at 1400 ℃ for 8 h

For complex permeability, the real part μ' (the ability for the storage of magnetic energy) and the imaginary part μ'' (the dissipation capacity of magnetic energy) have the same changing trend along with the rise of frequency from 2 to 18 GHz, as shown in Fig. 7a. Apparently, μ' and μ'' exhibit three distinct resonance peaks located at about 6.2, 11.6 and 16.6 GHz in turn, meaning perfect magnetic loss ability at these frequencies, which agree well with the magnetic loss tangent $\tan\delta_\mu$ determined by μ''/μ' (Fig. 7b). Generally, the magnetic loss contains exchange resonance, natural resonance and eddy current loss in the investigated frequency from 2 to 18 GHz. According to previous report, if the eddy current loss is the only reason for magnetic loss, frequency dependence of $C_0 = \frac{\mu''}{\mu'^2 f}$ should be a constant[21]. In Fig. 7c, C_0 is nearly constant with little fluctuation at the range of 5 ~ 18 GHz, suggesting that the eddy current loss dominates the magnetic loss but the exchange resonance may also exist. As for lower frequency between 2 and 5 GHz, the natural resonance will always dominate. For our YIG ceramic, values of $\tan\delta_\varepsilon$ and $\tan\delta_\mu$ were pretty low, indicating this is a low loss ceramic material which may be potential in DRA applications[12].

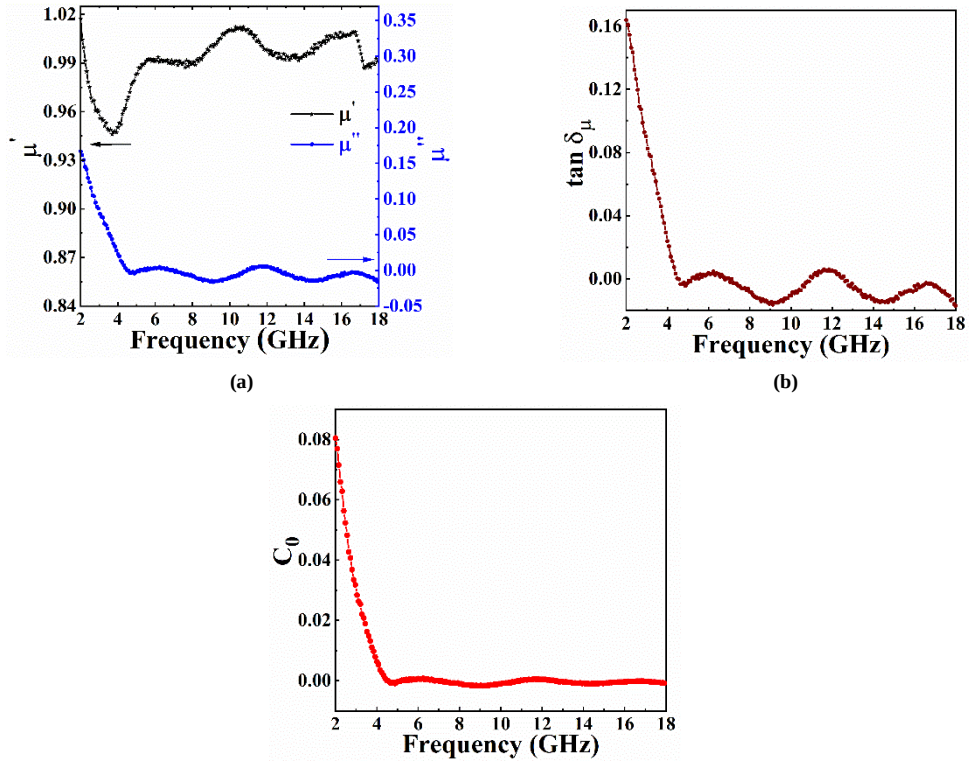

Fig. 7. Frequency dependence of (a) μ' and μ'', (b) tanδ_μ, (c) C_0 of YIG ceramic sintered at 1400 ℃ for 8 h

4 CONCLUSION

In this study, pure phase YIG ceramic was successfully produced by tape-casting forming process and one-step solid-state sintering method. The microstructure of the YIG ceramic fabricated at 1400 ℃ for 10 h showed a clear grain structure with an obvious grain boundary, and no pores were observed in the SEM images. At 1450 ℃ with the holding time of 8 h, the relative density of YIG ceramic was nearly 99.8%. The activation energy was calculated to be 183.81 kJ/mol. The saturation magnetization was 28.2 emu/g at 300 K. And, hysteresis loss at 30 K was as high as 238.8 mJ/kg, while values of that at 230 ~ 360 K were smaller than 10 mJ/kg. The zero-field complex permittivity properties show multiple dielectric relaxation loss, and the dielectric loss tangent tanδ_ε was nearly zero at 6 ~ 7 and 11 ~ 12 GHz. For complex permeability in the range of 5 ~ 18 GHz, the magnetic loss was mainly ascribed to the eddy current loss, and magnetic loss tangent tanδ_μ fluctuated at around zero. The low values of tanδ_ε and tanδ_μ indicate that it is a low loss ceramic material. This work provided a new fabrication method for much higher dense and purity fine-grained YIG ceramic. And the future work will be focused on the study of the uptown point (230 K) on the hysteresis loss chart, the dielectric properties under applied magnetic field in a wider range of frequency and the EMW absorption of the dense YIG ceramic.

REFERENCES

(1) Badahur, D. Current trends in applications of magnetic ceramic materials. *B. Mater. Sci.* **1992**, 15, 431–439.

(2) Adam, J. D.; Davis, L. E.; Dionne, G. F.; Schloemann, E. F.; Stitzer, S. N. Ferrite devices and materials. *IEEE T. Microw. Theory* **2002**, 50, 721–737.

(3) Nan, C.; Bichurin, M. I.; Dong, S.; Viehland, D.; Srinivasan, G. Multiferroic magnetoelectric composites: historical perspective, status and future directions. *J. App. Phys.* **2008**, 103, 031101–35.

(4) Huang, M.; Zhang, S. Y. Growth and characterization of rare-earth iron garnet single crystals modified by bismuth and ytterbium substituted for yttrium. *J. Mater. Chem. Phys.* **2002**, 73, 314–317.

(5) Huang, M.; Xu, Z. C. Liquid phase epitaxy growth of bismuth-substituted yttrium iron garnet thin films for magneto-optical applications. *Thin Solid Films* **2004**, 450, 324−328.

(6) Deschanvres, J. L.; Langlet, M.; Bochu, B.; Joubert, J. C. Growth of Bi-substituted YIG thin films for magneto-optic applications. *J. Magn. Magn. Mater.* **1991**, 101, 224−226.

(7) Kimzuka, N.; Katsura, T. Standard free energy of formation of $YFeO_3$, $Y_3Fe_5O_{12}$ and a new compound YFe_2O_4 in the Fe_2O_3-Y_2O_3 system at 1200 ℃. *J. Solid State Chem.* **1975**, 13, 176−181.

(8) Sánchez-De Jesús, F.; Cortés, C. A.; Valenzuela, R.; Ammar, S.; Bolarín-Miró, A. M.; Bolarin-Miro, M. Synthesis of $Y_3Fe_5O_{12}$ (YIG) assisted by high-energy ball milling. *Ceram. Int.* **2012**, 38, 5257−5263.

(9) Ali, W. F. F. W.; Othman, M.; Ain, M. F.; Abdullah, N. S.; Ahmad, Z. A. The investigation of the phenomenological YIG phase formation within 1000 ℃ to 1250 ℃: a kinetic approach. *J. Am. Ceram. Soc.* **2015**, 99, 315−323.

(10) Buscaglia, V.; Caracciolo, F.; Bottino, C.; Leoni, M.; Nanni, P. Reaction diffusion in the Fe_2O_3-Y_2O_3 system. *Acta Mater.* **1997**, 45, 1213−1224.

(11) Sztaniszláv, A.; Sterk, E.; Fetter, L.; Farkas-Jahnke, M.; Lábár, J. Investigation of garnet formation by sintering of Y_2O_3 and Fe_2O_3. *J. Magn. Magn. Mater.* **1984**, 41, 75−78.

(12) Ali, W. F. F. W.; Othman, M.; Ain, M. F.; Abdullah, N. S.; Ahmad, Z. A. The behavior of high frequency tunable dielectric resonator antenna (DRA) with the addition of excess Fe_2O_3 in $Y_3Fe_5O_{12}$ (YIG) formulation. *J. Mater. Sci-Mater. El.* **2014**, 25, 560−572.

(13) Ali, W. F. F. W.; Othman, M.; Ain, M. F.; Abdullah, N. S.; Ahmad, Z. A. Studies on the formation of yttrium iron garnet (YIG) through stoichiometry modification prepared by conventional solid-state method. *J. Eur. Ceram. Soc.* **2013**, 33, 1317−1324.

(14) Li, X.; Zhou, J.; Deng, J.; Zheng, H.; Zheng, L.; Zheng, P.; Qin, H. Synthesis of dense, fine-grained YIG ceramic by two-step sintering. *J. Electron. Mater.* **2016**, 45, 4973−4978.

(15) Chen, F.; Li, Q.; Wang, X.; Ouyang, J.; Nie, Y.; Feng, Z.; Gong, R.; Chen, Y.; Harris, V. G. Crystal structure tailored microwave magnetodielectric in $Yb_xY_{3-x}Fe_5O_{12}$ ceramic. *J. Alloy. Compd.* **2017**, 726, 1030−1039.

(16) Lide, D. R. *Vapor Pressure of the Metallic Elements. CRC Handbook of Chemistry and Physics.* 84th Edition, online version. CRC Press. Boca Raton, Florida **2003**, p309−313

(17) Ali, W. F. F. W.; Othman, M.; Ain, M. F.; Abdullah, N. S.; Ahmad, Z. A. Sintering and grain growth control of high dense YIG. *Ceram. Int.* **2016**, 42, 13996−14005.

(18) Fechine, P. B. A.; Silva, E. N.; Menezes, A. S.; Derov, J.; Stewart, J. W.; Drehman, A. J.; Vasconcelos, I. F.; Ayala, A. P.; Cardoso, L. P.; Sombra, A. S. B. Synthesis, structure and vibrational properties of $GdIG_x$:YIG_{1-x} ferrimagnetic ceramic composite. *J. Phys. Chem. Sol.* **2009**, 70, 202−209.

(19) Wu, H.; Liu, J.; Liang, H.; Zang, D. Sandwich-like Fe_3O_4/Fe_3S_4 composites for electromagnetic wave absorption. *Chem. Eng. J.* **2020**, 393, 124743-1−13.

(20) Zou, J.; Wang, Z.; Yan, M.; Bi, H. Enhanced interfacial polarization relaxation effect on microwave absorption properties of submicron-sized hollow Fe_3O_4 hemispheres. *J. Phys. D: Appl. Phys.* **2014**, 47, 275001−9.

(21) Lan, D.; Qin, M.; Yang, R.; Chen, S.; Wu, H.; Fan, Y.; Fu, Q.; Zhang, F. Facile synthesis of hierarchical chrysanthemum-like copper cobaltate-copper oxide composites for enhanced microwave absorption performance. *J. Colloid Interface Sci.* **2019**, 533, 481−491.